SHearography for the **I**nspection of **C**omposites – Phase 2 (**SHIC2**)

Grant No. 0050.0084943.13.9

PIPELINE BONDED JOINTS ASSEMBLY AND OPERATION HEALTH MONITORING WITH EMBEDDED FBG SENSORS

Authors: Thiago Destri Cabral*, Antonio Carlos Zimmermann, Daniel Pedro Willemann, and Armando Albertazzi Gonçalves Jr.

*tdcabral@ifi.unicamp.br

Presented at: **7th International Electronic Conference on Sensors and Applications (ECSA-7)**

15/11/2020 - 30/11/202

Presentation Summary

1. Introduction
2. Test Specimen and Instrumentation Design
3. Test Specimen Assembly
4. Results and Discussion
5. Conclusion

1. Introduction

The use of fiber reinforced plastics (FRP) pipelines with bonded joints is increasingly more common:

- Produced water in offshore oil platforms, gas lines, etc.;
- Joint failure disrupts operation causing significant financial losses and, possibly, severe environmental contamination.

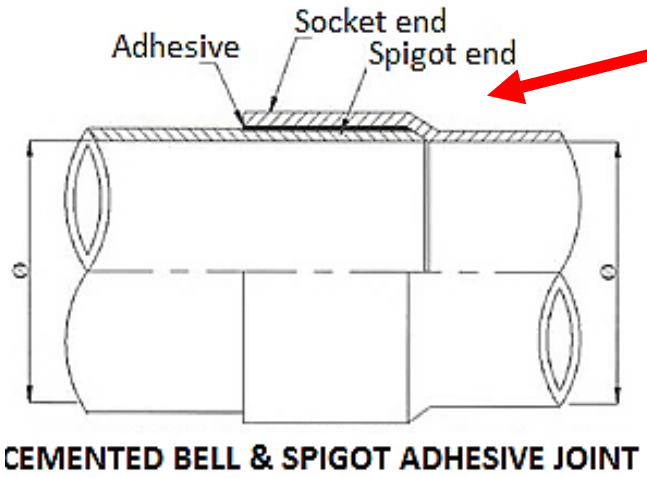

CEMENTED BELL & SPIGOT ADHESIVE JOINT

[Images Source: NOV Ameron]

1. Introduction

This creates the demand for monitoring and inspection:

- To ensure structural integrity;
- To increase security and minimize downtime.

Standards for bonded joint inspection such as Norsok M-622, ISO 14692-4 and NBR 15921-4 make use of hydrostatic testing, ultrasound testing and radiography:

- Applicable to only certain stages of the pipeline lifecycle;
- Can be difficult to execute on the field (harsh conditions, confined spaces);
- No long-term monitoring capability.

An integrated instrumentation approach offers promising prospects:

- Reduced costs;
- Does not disrupt operation;
- Diagnosis and prognosis capabilities;
- Can monitor hard to reach locations;
- Integrated sensors are protected from ambient conditions;
- Capable of long-term monitoring.

1. Introduction

Research proposal: Integrated instrumentation for axial strain monitoring using fiber optic sensors embedded into the adhesive layer of bonded joints.

- Fiber optic sensors offer inherent advantages:
  - Small dimensions -> low impact on joint mechanical properties;
  - Immunity to electromagnetic interference;
  - No electrical power needed -> Increased security for oil and gas;
  - High multiplexing capability -> Multiple sensors per fiber.
  - Anomalies on the strain levels indicate the presence of defects;
  - Effective from joint assembly to pipeline operation.

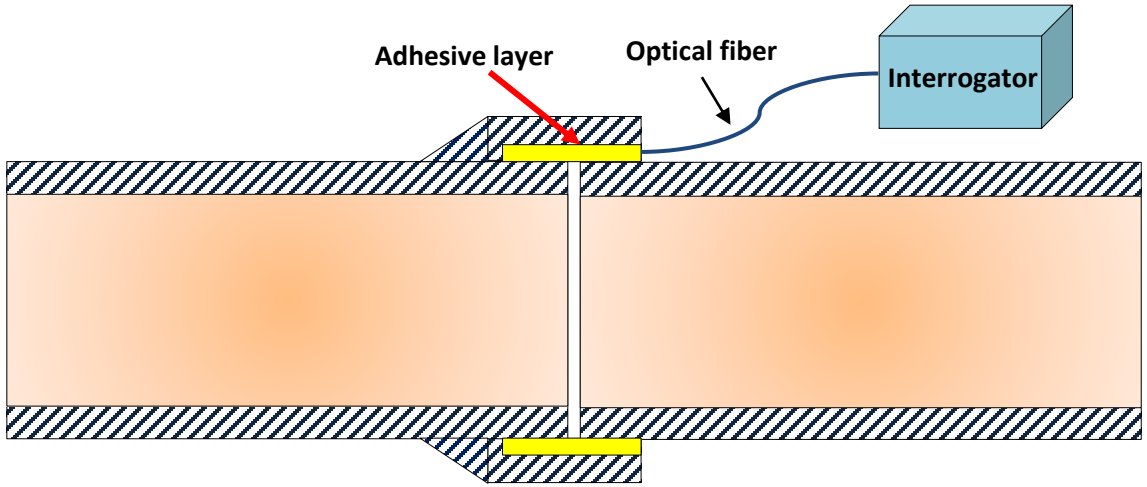

2.1. Test Specimen Design

For the experiments, several test specimens were assembled using Chlorinated Polyvinylchloride (CPVC) industrial grade (Schedule 80) pipes and fittings:

- 4” nominal diameter;
- Comprised of 2 straight pipe sections joined by a sleeve;
- One section is terminated with an endcap;
- The opposite section is fitted with a flange;
- Flange and endcap are solvent welded, while sleeve is adhesive bonded with industrial grade bi-component methyl-methacrylate adhesive;
- Insertion depth recommended by the manufacturer is 57 mm, stress concentration is expected in 2 regions as shown in the diagram below.

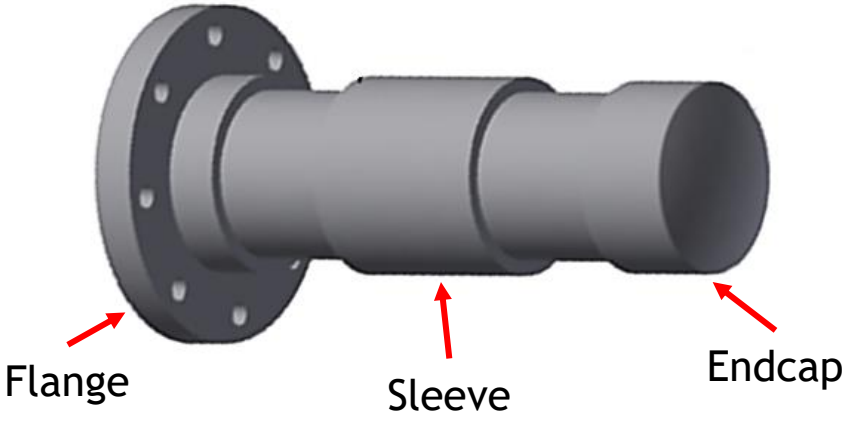

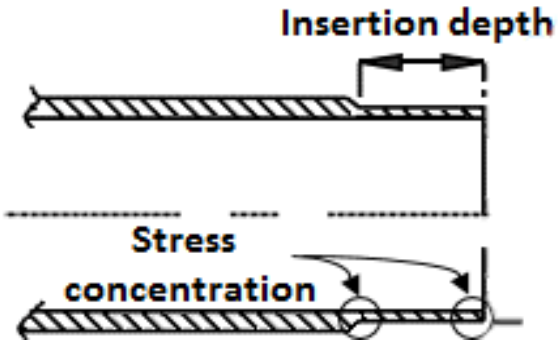

2.2 Instrumentation Design

Fiber Bragg Gratings (FBGs) were selected for use in this study:

- Relatively simple, ample technical literature available, high applicability in structural health monitoring;
- Consists of a periodic modulation of the refractive index in the fiber core;
- When a broadband light signal is transmitted down the fiber a narrowband reflection with a well-defined peak wavelength λ_B is observed:

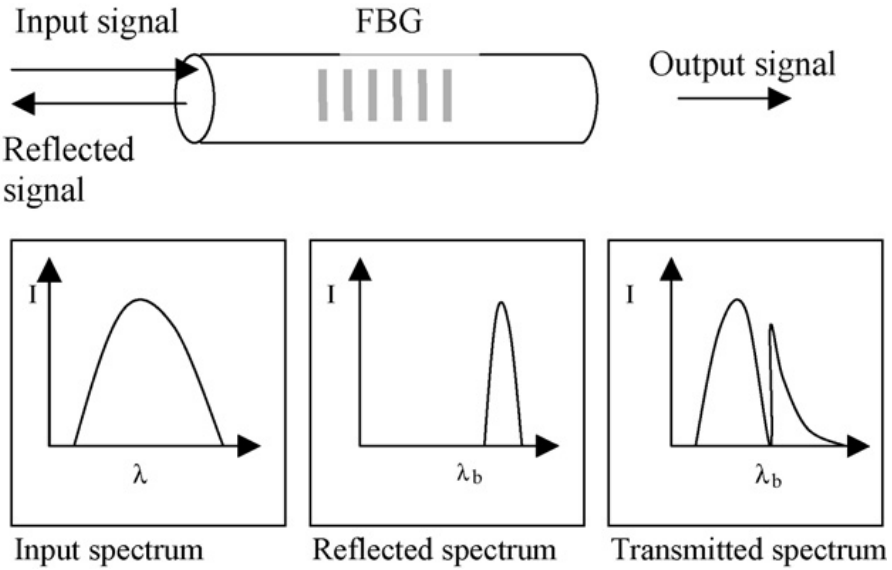

[Source: Majumder et. al. – doi.org/10.1016/j.sna.2008.04.008]

2.2 Instrumentation Design

λ_B is given by the Bragg condition: $\lambda_B = 2.n_{ef}.\Lambda$

- λ_B → Bragg wavelength;
- n_{ef} → Refractive index of the fiber core for the fundamental mode;
- Λ → Period of the refractive index modulation

The FBG is sensitive to temperature and strain, as they affect n_{ef} and Λ:

$$\frac{\Delta\lambda_B}{2} = \left[\left(\Lambda\frac{\delta n_{ef}}{\delta L} + n_{ef}\frac{\delta\Lambda}{\delta L}\right)\Delta L + \left(\Lambda\frac{\delta n_{ef}}{\delta T} + n_{ef}\frac{\delta\Lambda}{\delta T}\right)\Delta T\right]$$

$$\frac{\Delta\lambda_B}{\lambda_B} = K_\varepsilon\Delta\varepsilon + K_T\Delta T$$

$K_\varepsilon = 7{,}64x10^{-6}$

$K_T = 0{,}769$

(typical values)

In this work we performed all experiments under a controlled temperature environment to eliminate its effect in the strain measurements.

2.2 Instrumentation Design

To assess strain levels around both strain concentration points and in-between them, sensing fibers with 3 strain sensors (Fiber Bragg Gratings) were devised:

- Standard SMF-28 fibers with polyimide coating;
- 0.9 mm diameter Teflon loose tube protects non-embedded fiber length;
- Standard FC/APC connector;
- Each FBG in a fiber has a distinct nominal wavelength;
- $\lambda_{B1} < \lambda_{B2} < \lambda_{B3}$ facilitates identifying the location of each FBG during interrogation;
- Separation between λ_Bs is ≥ 5 nm to avoid overlap due to non-uniform loading.

Schematic drawing of the sensing fiber (dimensions in mm):

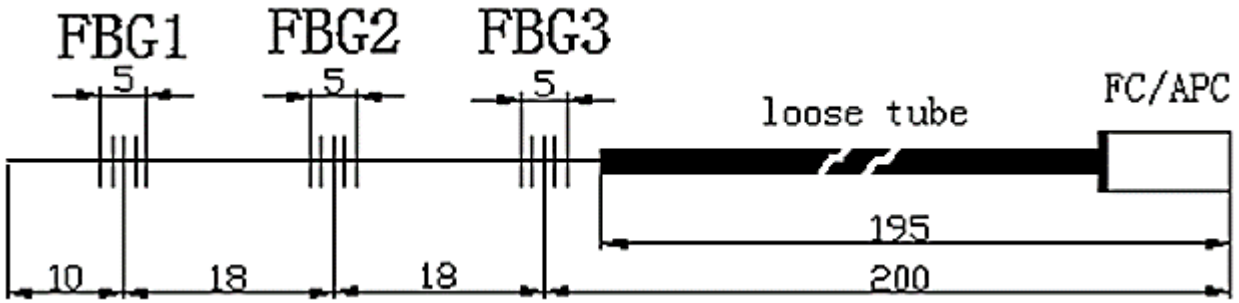

3. Test Specimen Assembly

Firstly the sensing fibers are pre-positioned using adhesive tape, note that FBG1 will be the one embedded the deepest into the bonded joint, with FBG 3 closer to the exit point from the adhesive layer:

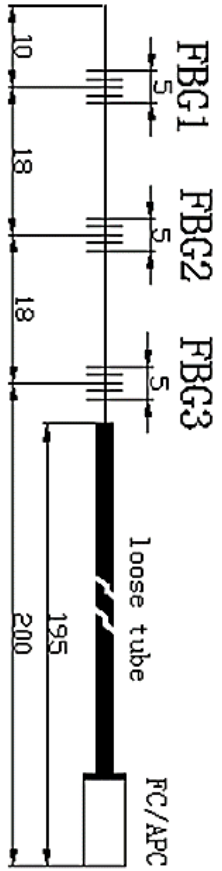

3. Test Specimen Assembly

A droplet of cyanoacrylate adhesive is used to secure the tip of the fiber to the wall of the pipe, avoiding bending or breakage of the fiber during embedding:

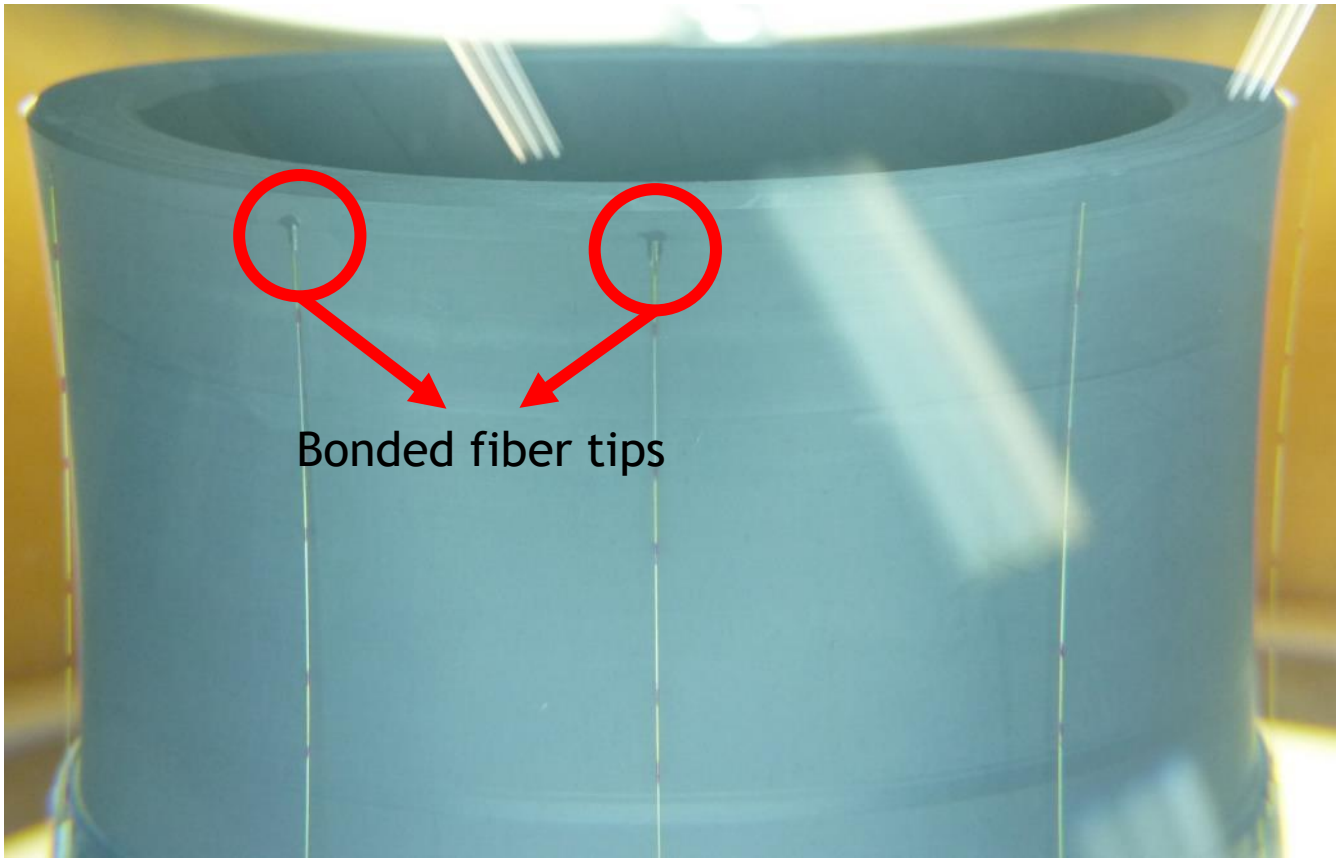

3. Test Specimen Assembly

The methyl-methacrylate adhesive is then firstly applied along the fibers to further secure them in place:

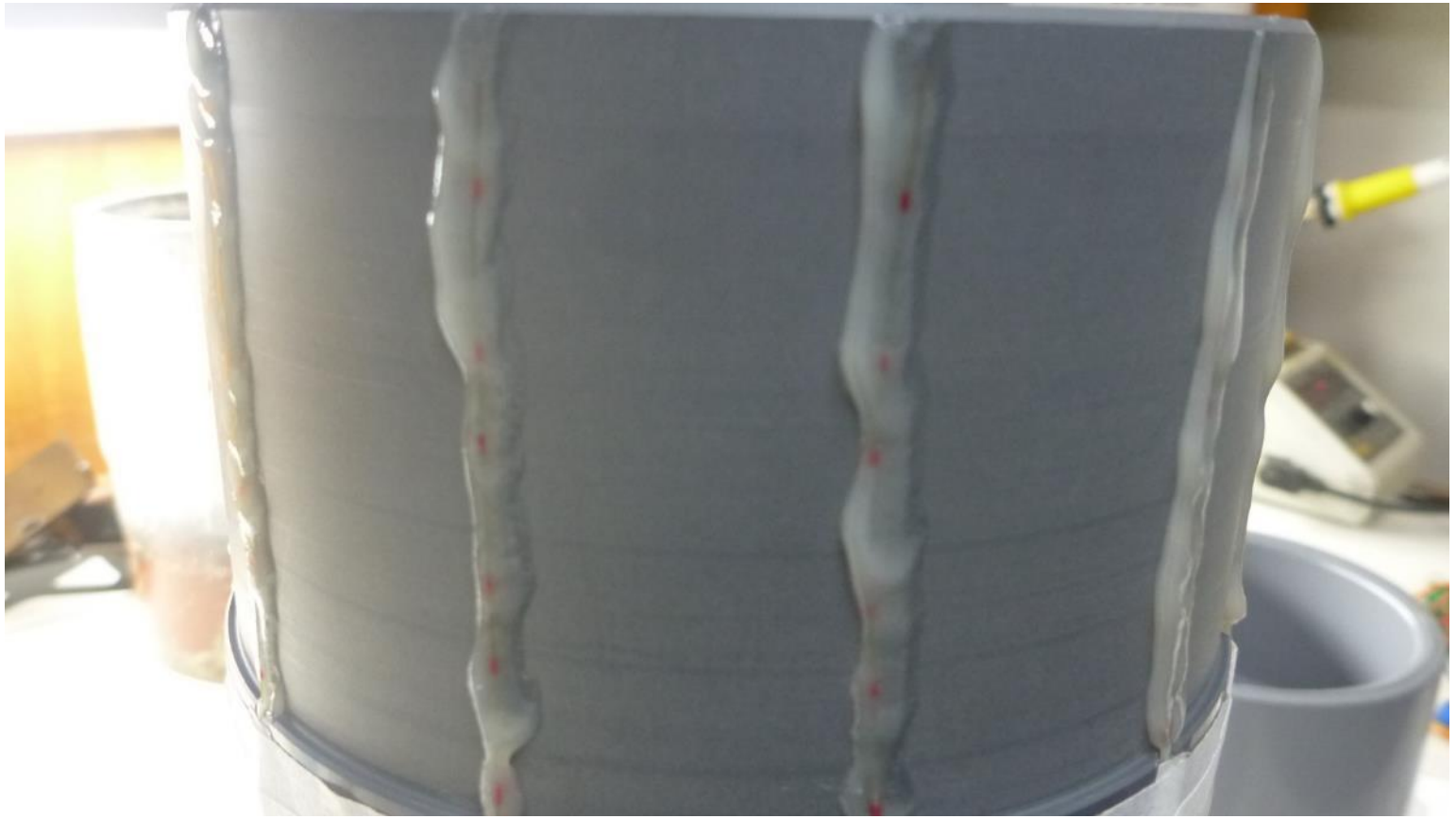

3. Test Specimen Assembly

And then applied liberally to the whole area to be inserted into the sleeve:

3. Test Specimen Assembly

Adhesive is also applied to the inner side of the sleeve:

3. Test Specimen Assembly

Both parts are carefully brought together and once the adhesive is fully cured the integrity of the embedded sensors is checked:

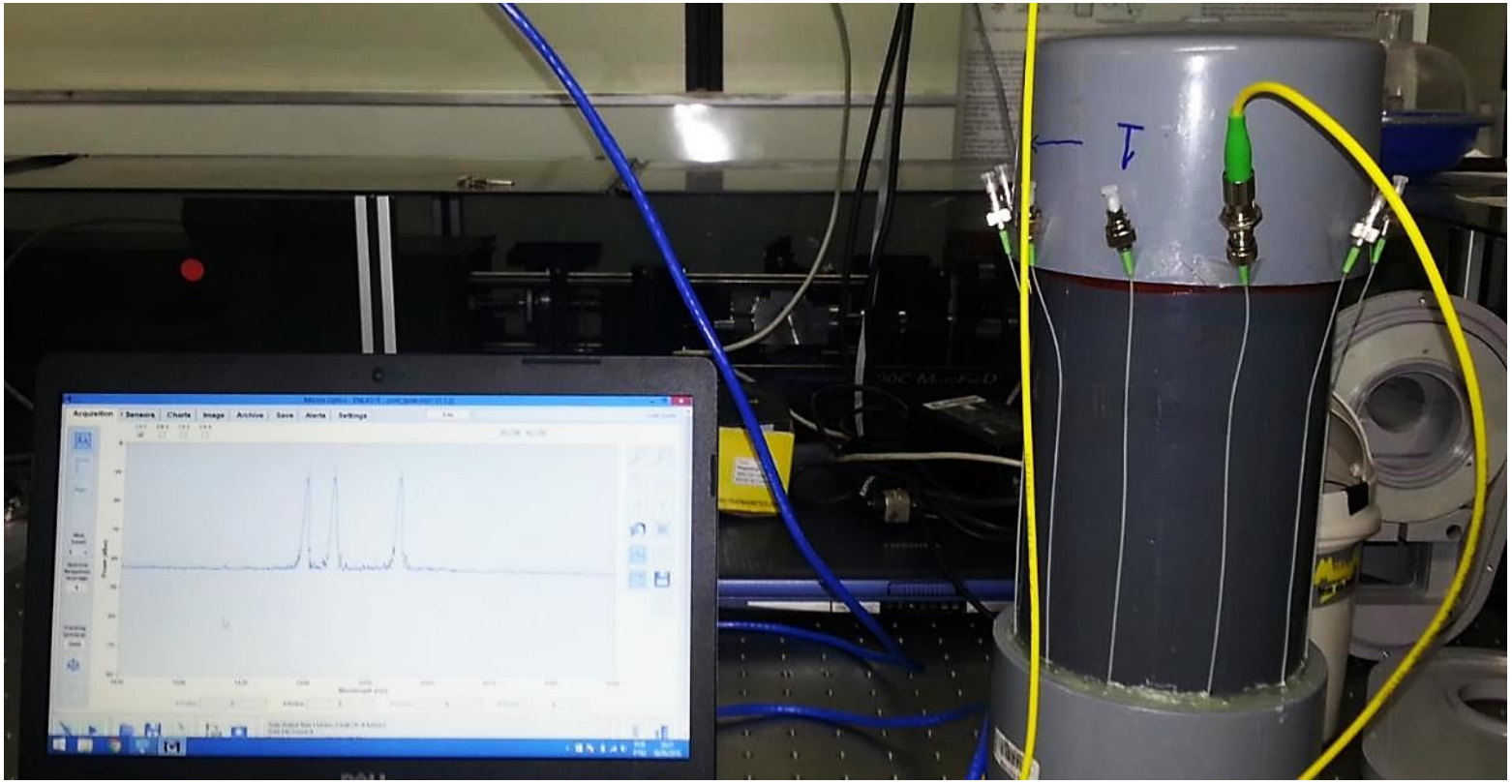

3. Test Specimen Assembly

Intentional defects were introduced in one of the test specimens using Teflon sheets with aluminum tape (to increase detectability by tomography), which prevents proper adhesion and load transfer between the pipe and the sleeve:

3. Test Specimen Assembly

A total of 3 test specimens were assembled, that will be referred as S1, S2 and S3 in this presentation:

- S1 was prepared with a severe lack of adhesive;
- S2 was prepared to be as structurally sound as possible;
- S3 contains the intentional effects;
- The instrumented bonded joint of all specimens were subjected to a computed tomography test;
- A total of 12 fibers were planned to be embedded per joint. Considering the pipe dimensions this results in a 43.6 mm circumferential separation between fibers. This was accomplished for S2 and S3, but S1 has only 11 fibers due to a defective sensing fiber, resulting in a 47.6 mm separation between sensing fibers for S1.

4. Results and Discussion

By reconstructing the bonded joint geometry from the computed tomography data it can be observed:

- Widespread lack of adhesive (darker areas) in S1;
- No major defects, but the presence of porosity (darker spots) in S2;
- Some porosity (darker spots) in S3, with the intentionally embedded defects clearly outlined (arrows);

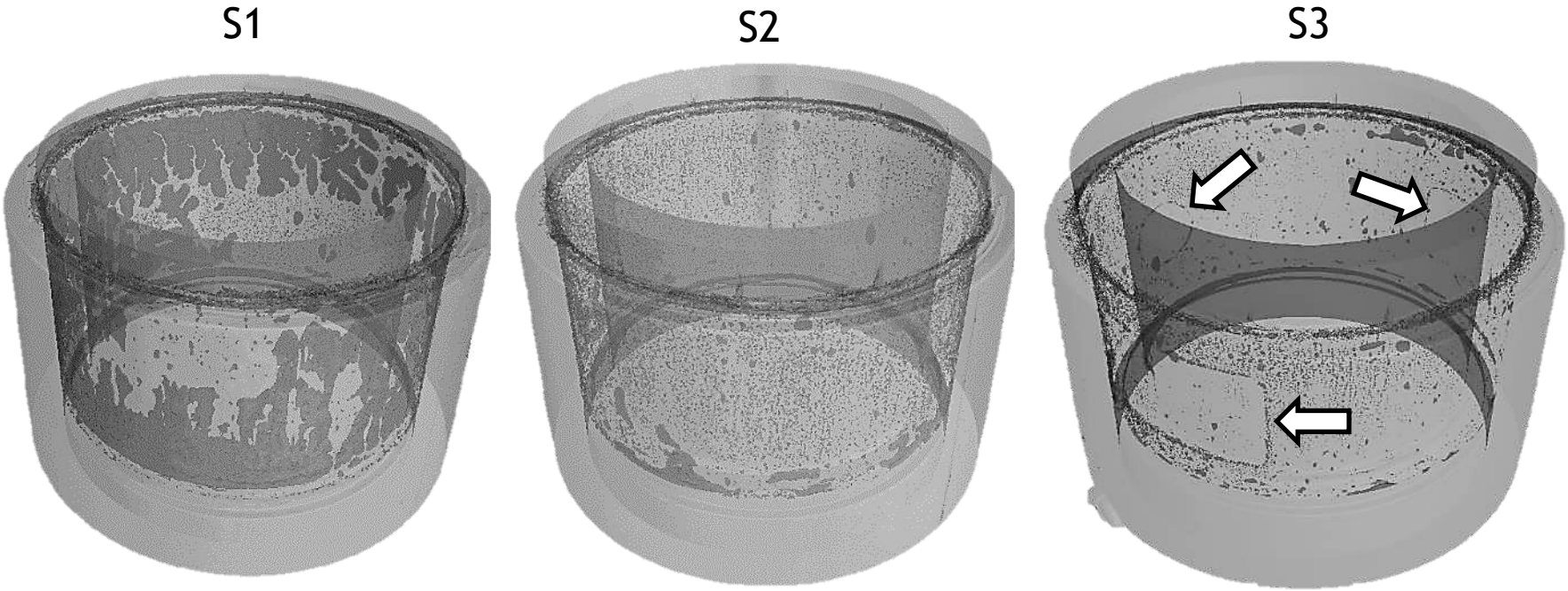

4. Results and Discussion

The first test executed with the sensors was adhesive cure strain, corresponding to obtaining strain data for the FBGs after the adhesive is fully cured. In this test we compare results from all test specimens:

- This test corresponds to monitoring the lifecycle stage of assembly of the joint and is a critical point as is during this stage that defects are embedded due to improper assembly procedures;

- Strain map is expected to be entirely negative (compressive strain), as the adhesive shrinks as it cures;
- Data is represented in 3D surface maps (bilinear interpolation of FBG data) and a corresponding colormap (top view of surface plot);

- Note that the FBG axis and the Optical Fiber axis both start at 0 in the graphics, and as such FBG1, FBG2 and FBG3 from the previous schematic drawing correspond to 0, 1, and 2 in the maps;
- Similarly, the last entry in the Optical Fiber axis is a repeat of the data for the 0^{th} line to completely represent the full circumference of the joint.

4. Results and Discussion

Adhesive curing strain data for S1 is shown below:

- As can be observed, strain levels fluctuate intensely, and positive (tensile) strain is observed;
- No circumferential symmetry (Optical Fiber axis) is observed in the data, which would be expected in a tubular symmetrical structure;
- These observations can be attributed to the widespread lack of adhesive causing a non-uniform strain distribution in the adhesive layer

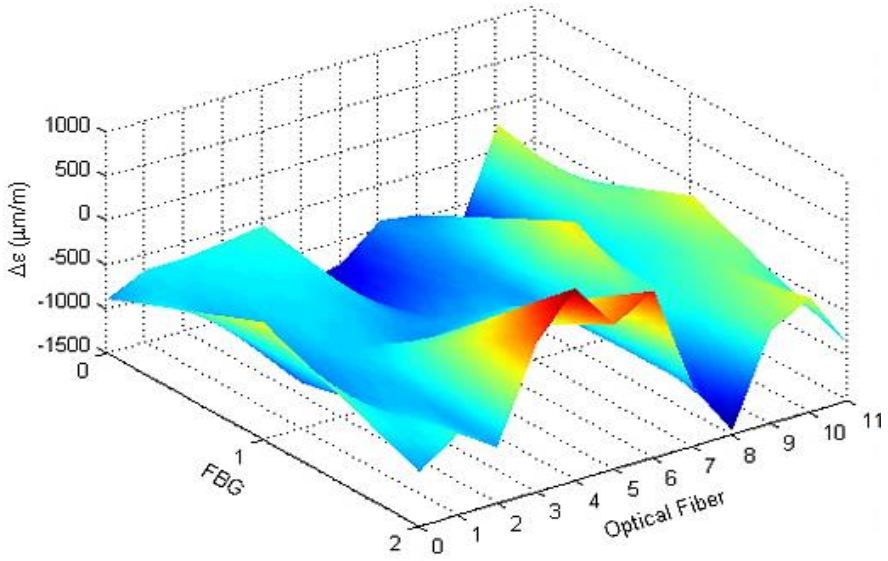

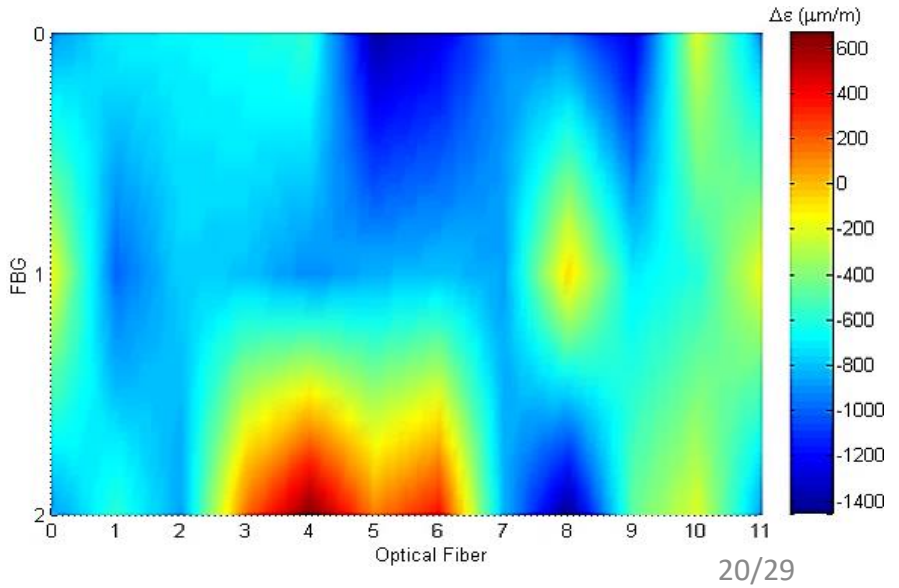

4. Results and Discussion

Adhesive curing strain data for S2 is shown below:

- Only negative (compressive) strain is observed, along with very good level of circumferential symmetry;
- Strain is more intense towards the outer edge of the joint, as is expected when considering strain concentration and the transition to a region with less material to resist stresses (bare pipe as opposed to pipe + sleeve);
- The curing strain maps shows clear differences between a sound joint and one with severe lack of adhesive defects.

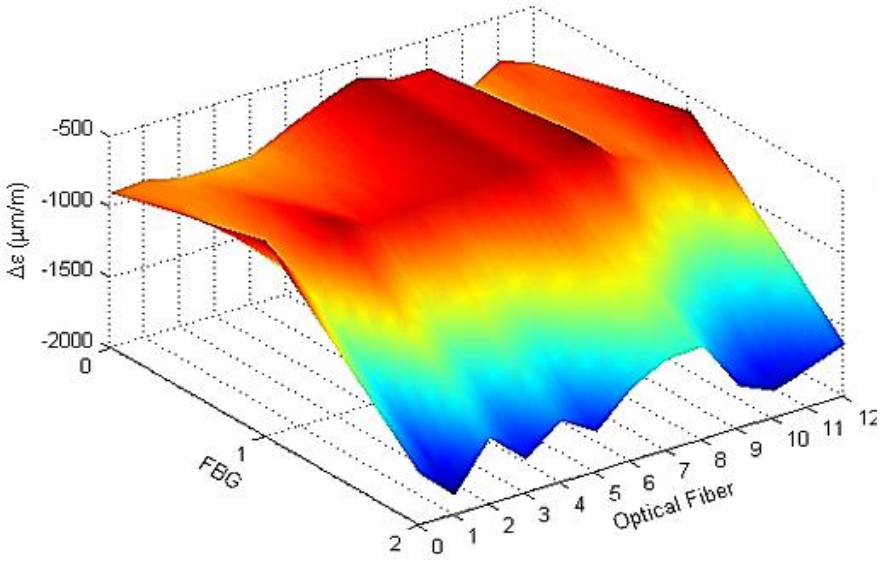

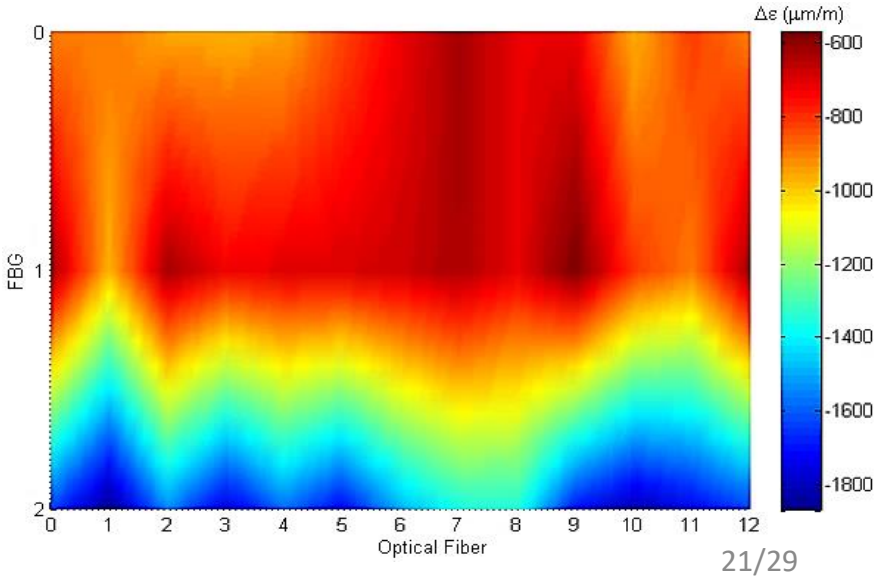

4. Results and Discussion

Adhesive curing strain data for S3 is shown below:

- Only negative (compressive) strain is observed, but the symmetry observed in S2 is not present;
- Strain artifacts are observed mostly around the position of planned defects (black dashed lines, stretching is caused by image aspect ratio), more evidently around the larger rectangular defect;
- The curing strain maps shows clear differences between a sound joint (S2) and one with moderately sized lack of adhesive defects (S3), which could be used as a base to flag this joint for further inspection.

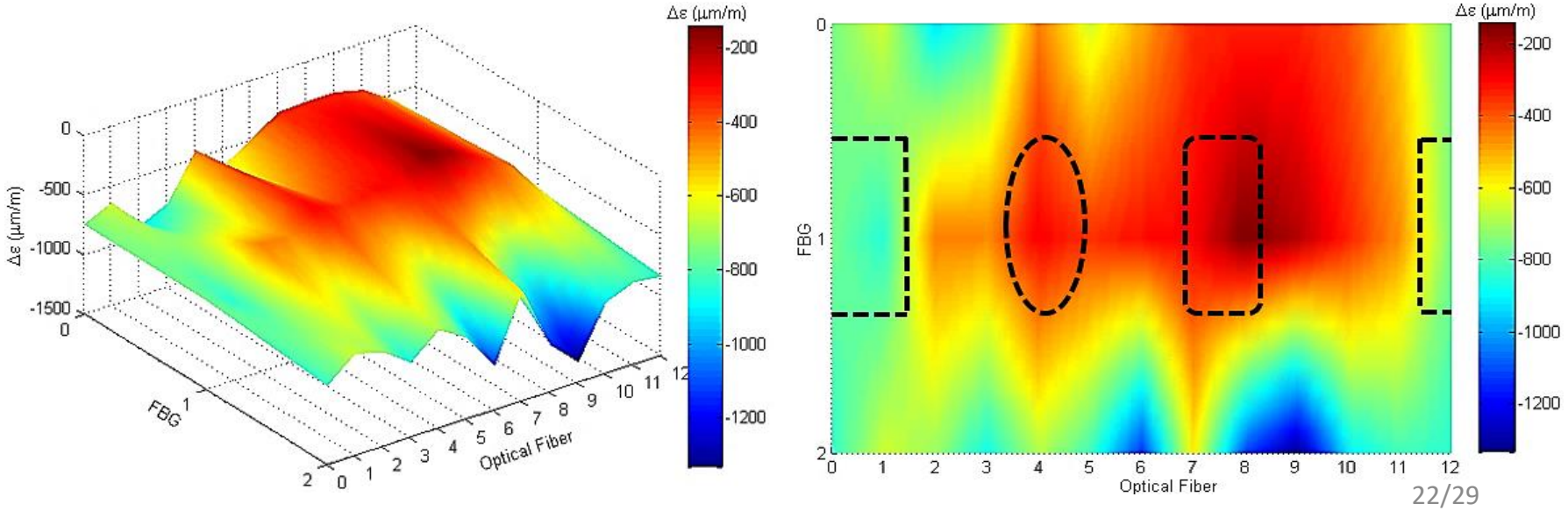

4. Results and Discussion

Next the fully assembled and water filled test specimens were prepared for hydrostatic testing, but the setup allows for preforming a flexural load test:

- Observing the picture of the prepared test specimen below, we see that it is being supported from below in 3 points (endcap, before and after the sleeve, pointed by the arrows);
- The setup creates a slight flexural load in the sleeve, with the maximum load roughly centered in the middle of the sleeve;
- This creates the opportunity to simulate the introduction of slight flexural loads by rotating the test specimen around its long axis, obtaining strain maps before and after the rotation and computing $\Delta\varepsilon$ between both maps.

4. Results and Discussion

Flexural load $\Delta\varepsilon$ data for S2 is shown below:

- The strain profile is clearly in line with the expected for a flexural load, with negative and positive strain in opposite sides of the joint;
- Very slight strain levels ($-20 < \mu\varepsilon < 50$) were detected with basically no noise, showing this setup is very sensitive and accurate;
- This shows that this setup can also be used to monitor stresses introduced during the pipeline assembly stage of the pipeline lifecycle, when correcting misalignments between different pipeline sections to be joined.

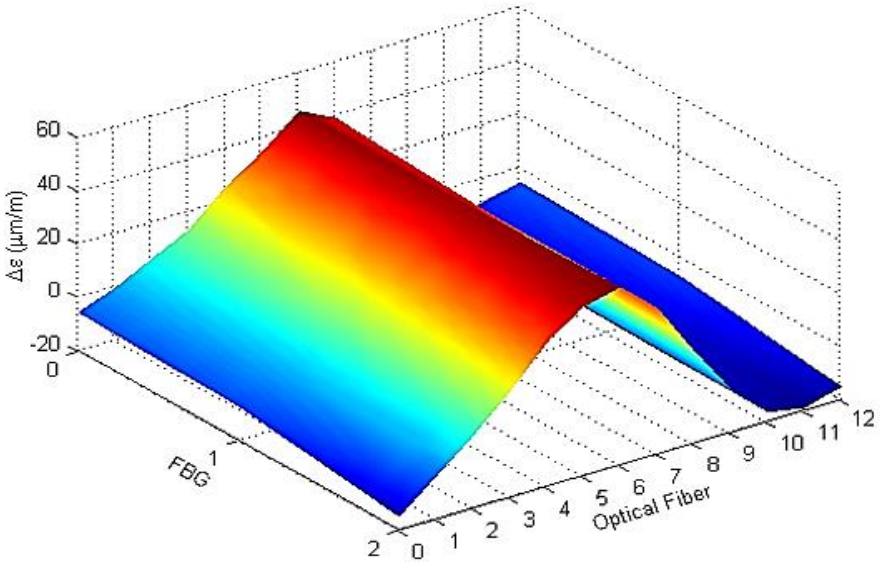

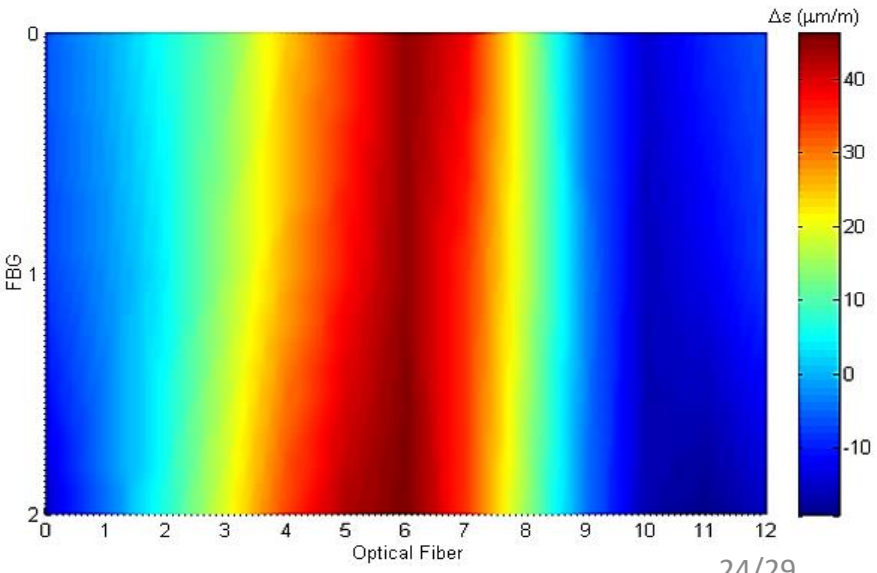

4. Results and Discussion

Similarly as observed for the adhesive curing strain test, if we compare flexural strain maps for S2 (left) and S3 (right), even though the strain artifacts do not clearly highlight the position of possible defects (black dashed lines), a strong enough deviation from what is expect from a sound joint is observed in S3 to warrant flagging it for further inspection in a real application scenario.

This further demonstrates the capability of the proposed setup to detect the presence of defects in bonded joints on different stages of the pipeline lifecycle.

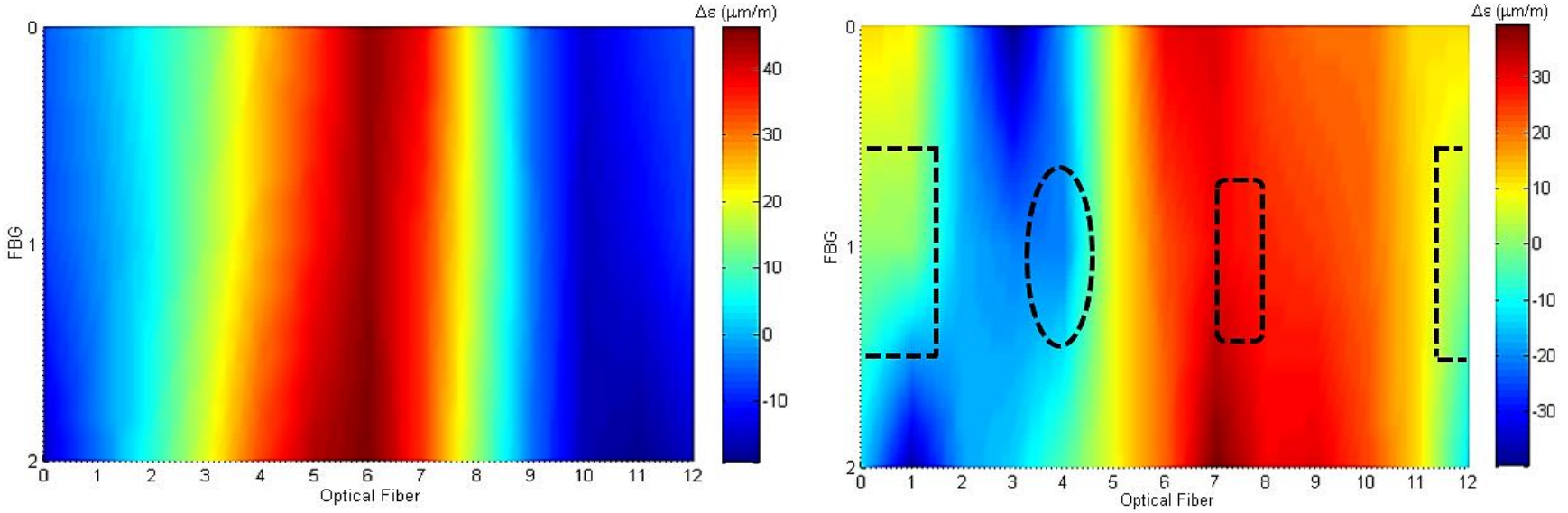

4. Results and Discussion

Finally, hydrostatic testing was performed. In this test we compare the results from S2 and S3.

- This test corresponds to detecting and monitoring the presence of defects during the operation stage of the pipeline lifecycle;

- Strain map is expected to be entirely positive (tensile strain), as the test specimens expand in the axial direction since it is closed in both ends;

- Strain maps shown correspond to $\Delta\varepsilon$ computed by comparing sensor data for the unpressurized pipe and data collected for a manometric internal pressure load of 7 bar (0.7 MPa).

4. Results and Discussion

Hydrostatic strain data for S3 ($\Delta P = 7$ bar) is shown below:

- Position of intentional defects is outlined by the black dashed lines in the color map (stretching is caused by image aspect ratio);
- Interesting strain artifacts can be observed in the position of the circular defect and around the larger rectangular defect;
- The smaller square defect, positioned in between fibers, as opposed to the other 2 defects placed on top of FBGs, did not cause a large enough disturbance in the strain field to be observable.

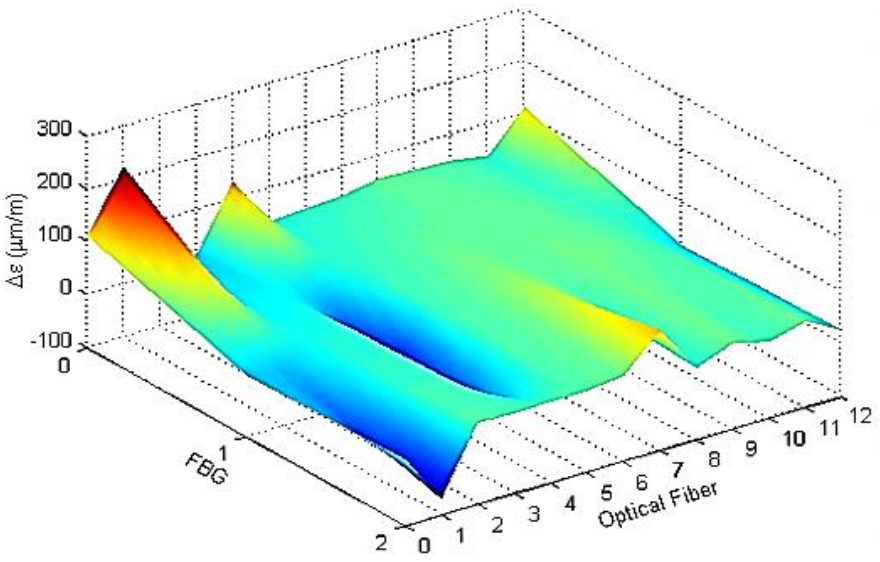

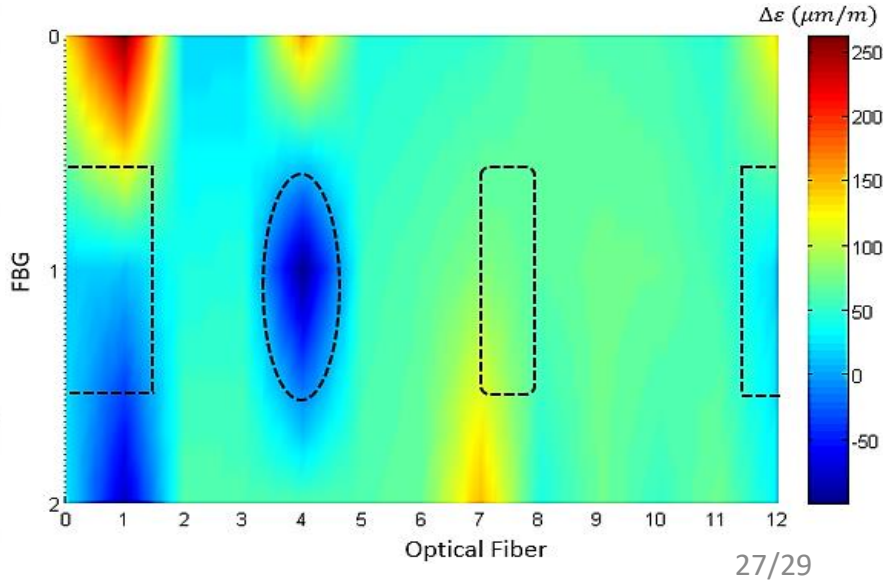

4. Results and Discussion

Hydrostatic strain data for S2 ($\Delta P = 7$ bar) is shown below:

- Only tensile strain is observed;
- While some fluctuation in the strain level is observed, it is relatively small (mean strain = 79.5 $\boldsymbol{\mu\varepsilon}$, standard deviation = 13.4 $\boldsymbol{\mu\varepsilon}$);
- The fluctuations are mostly likely caused by porosity around the FBG sensors, as observed in the tomography reconstruction of S2's bonded joint;
- To better illustrate how small these fluctuations are compared to the ones caused by larger defects like in S3, the color bar for the colormap of S2 below has been rescaled to match that of S3.

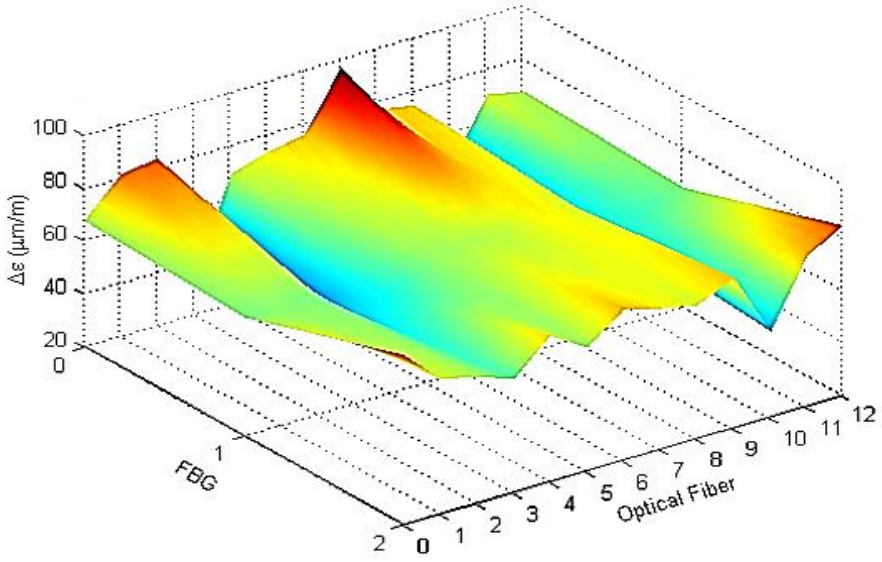

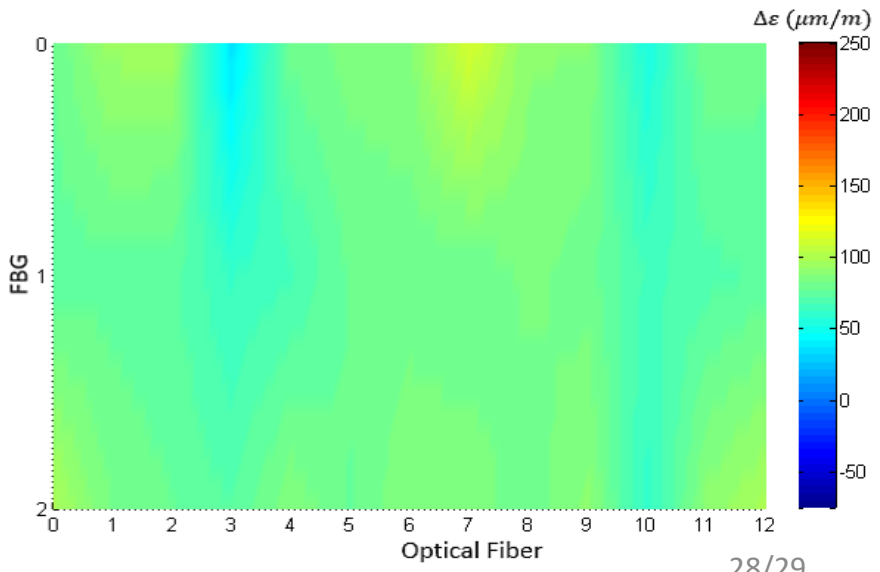

5. Conclusions

• A sensing setup to detect and monitor defects in bonded joints between pipelines by measuring axial strain in the adhesive layer with embedded FBG sensors was demonstrated.

• The setup was shown adequate to monitor the assembly of the joints, assembly of the pipelines, and the pipeline operation, effectively covering all stages of the pipeline lifecycle after manufacturing of the individual parts themselves.

• Although further studies are needed before practical field measurements can be realized, e.g. developing strategies for compensating temperature effects on the FBG sensor data, the achieved results of this work are very promising and can find ample use for monitoring plastic and composite pipelines that make use of adhesive bonded joints.

Thank you for your attention,

Questions?